NACA

RESEARCH MEMORANDUM

WIND-TUNNEL INVESTIGATION OF THE USE OF LEADING-EDGE AND
TRAILING-EDGE AREA-SUCTION FLAPS ON A 13-PERCENT-THICK
STRAIGHT WING AND FUSELAGE MODEL

By Curt A. Holzhauser

Ames Aeronautical Laboratory Moffett Field, Calif.

NATIONAL ADVISORY COMMITTEE FOR AERONAUTICS

WASHINGTON

January 24, 1958 Declassified September 17, 1958

NATIONAL ADVISORY COMMITTEE FOR AERONAUTICS

RESEARCH MEMORANDUM

WIND-TUNNEL INVESTIGATION OF THE USE OF LEADING-EDGE AND
TRAILING-EDGE AREA-SUCTION FLAPS ON A 13-PERCENT-THICK
STRAIGHT WING AND FUSELAGE MODEL

By Curt A. Holzhauser

SUMMARY

A wind-tunnel investigation was undertaken to determine the effectiveness of area suction in increasing the lift of a moderately thick straight wing which encountered trailing-edge type of air flow separation. The wing had a partial-span trailing-edge flap and a full-span leading-edge flap, both with porous area at the knee. The results indicated that area suction increased the trailing-edge flap lift increment at 0° angle of attack to about 90 percent of the theoretical value. The flap lift increment decreased with increasing angle of attack, presumably because of trailing-edge air-flow separation, and a maximum lift coefficient of 1.9 was obtained with the undeflected leading-edge flap. Deflecting the leading-edge flap and applying suction increased the maximum lift coefficient to 2.4. However, the full effectiveness of the leading-edge area-suction flap was not obtained because of trailing-edge air-flow separation that occurred on the wing.

INTRODUCTION

Experimental investigations have demonstrated that area suction can increase the lift coefficients obtainable with swept wings and thin unswept wings. It was found that area suction at the knee of the trailing-edge flap delayed separation from the knee to high flap deflections with a resulting increase in the flap lift increment (refs. 1 through 7). When area suction was applied at the leading edge or leading-edge flap of the wings tested, the air-flow separation from the forward portion of the wing was delayed to high angles of attack with resulting improvements in lift, drag, and pitching-moment characteristics of the model (refs. 1, and 5 through 10).

All of these large-scale, three-dimensional tests with area suction were performed with wings for which the maximum lift was limited by leading-edge type of air-flow separation. Since it was not known whether trailing-edge type of air-flow separation would reduce the effectiveness of area suction, an investigation was undertaken with a wing that would be expected to encounter trailing-edge separation. The model had a fuselage and a straight, 13-percent-thick wing with leading-edge and trailing-edge flaps having porous area at the knee of the flaps. Tests were first made to evaluate the effectiveness of area suction when applied to the partial-span trailing-edge flaps; for these tests, the leading-edge flap was undeflected. Tests were then made with the area-suction leading-edge flap and with the trailing-edge flap deflected and undeflected. The results of this experimental investigation which was conducted in the Ames 40- by 80-foot wind tunnel are reported herein.

NOTATION

b wing span, ft

c chord of wing, ft

 $\frac{1}{c}$ mean aerodynamic chord, $\frac{2}{S} \int_{c^2 dy}^{b/2} c^2 dy$, ft

 C_D drag coefficient, $\frac{drag}{qS}$

 C_{L} lift coefficient, $\frac{\mathrm{lift}}{\mathrm{qS}}$

 $^{\mathrm{C}}\mathrm{L}_{\delta_{1}}$ rate of change of lift increment per unit deflection of a full-chord flap

 $riangle ext{L}_{ ext{F}}$ increase in lift coefficient when trailing-edge flap was deflected at $ext{O}^{ ext{O}}$ angle of attack

 C_m pitching-moment coefficient referred to $\frac{\overline{c}}{\mu}$, $\frac{\text{pitching moment}}{q\overline{c}S}$

 C_Q flow coefficient, $\frac{W}{\rho gUS}$

g acceleration of gravity, 32.2 ft/sec²

L.E. leading edge

- p free-stream static pressure, lb/sq ft
- pd duct static pressure, lb/sq ft
- P_d duct pressure coefficient, $\frac{p_d p}{q}$
- q free-stream dynamic pressure, lb/sq ft
- S wing area, sq ft
- U free-stream velocity, ft/sec
- W weight rate of flow, lb/sec
- angle of attack, referred to fuselage center line, deg
- δ flap deflection, deg
- $\frac{d\alpha}{d\delta}$ lift effectiveness parameter, $\frac{c_{L_{\delta}}}{c_{L_{\tau}}}$
- ρ mass density of air at standard conditions, 0.002378 slugs/cu ft

Subscripts

crit critical

F trailing-edge flap

N leading-edge flap

MODEL AND APPARATUS

A photograph of the model mounted in the test section of the Ames 40- by 80-foot wind tunnel is presented in figure 1. The over-all dimensions of the model are given on the three-view drawing in figure 2.

The wing had an aspect ratio of 6, taper ratio of 0.38, and 0° of sweep measured at the 52-percent chord line. The wing had 3.8° of dihedral with 1.5° of twist. The root of the wing was set on the center line of the fuselage with 1° of incidence. The coordinates of the airfoil

section, an NACA 651213 (a = 0.5), are given in table I. A 14-percent-chord leading-edge flap extended across the full span of the exposed wing, and a 25-percent-chord trailing-edge flap extended from the 20 to the 56 percent semispan station. The leading-edge flap deflection could be maintained at any value from 0° to 40°; whereas, the trailing-edge flap could only be deflected either 45° or 55°. The leading- and trailing-edge flaps had porous area at the knee to form a plain-type flap (see fig. 3). This porous area, constructed from an outer surface of electroplated mesh screen backed by wool felt, had the pressure-flow characteristics shown in figure 4. The extent of porous area for all flap configurations was controlled with a nonporous tape about 0.003 inch thick. A limited number of pressure orifices were located on the surfaces of the wing, flaps, and porous areas, and in the flap ducts.

For selected configurations vortex generators were taped to the upper surface of the wing at the locations shown in figure 5. These vortex generators were 2 inches square, and they were set at an angle of 15°0 with respect to the fuselage center line.

Coordinates for the wing tip tanks, shown in figures 1 and 2, are given in table II. When these tanks were removed, the wing span was 37 feet 6 inches, and the exposed wing tips were approximately square.

The width and depth of the fuselage are given in table III for several stations. This fuselage contained the plenum chamber and pumping equipment. The suction flow for the leading-edge and trailing-edge flaps was provided by a compressor driven by variable-speed electric motors. The flow in each of the flaps was controlled by an electrically actuated valve. The flow quantities through each of the ducts was determined by a total- and a static-pressure tube, corrected by factors determined from calibrations made with a standard ASME orifice meter.

TESTS, PROCEDURE, AND CORRECTIONS

The leading- and trailing-edge flap deflections and porous extents that were tested are listed in table IV. Lift, drag, pitching moment, suction flow quantities, and duct pressures were measured for all of these configurations. The tests were performed for an angle of attack range of -4° to 29° at an angle of sideslip of 0° . The tunnel airspeed was maintained at 112 feet per second which corresponded to a Reynolds number of 4.8×10^{6} , based on the mean aerodynamic chord.

Tests were first performed at a fixed angle of attack with various suction quantities to determine the associated lift, flow, and duct pressure coefficients. Figure 6 shows the variation of lift coefficient with flow coefficient obtained for two deflections of the trailing-edge

NACA RM A57KOl 5

flap with the model at 0° angle of attack. As in previous area-suction investigations, the lift coefficient first increased rapidly with increasing flow coefficient, reaching a point beyond which the lift coefficient increased very slowly. The point at which this change occurred has been referred to as the critical point (ref. 1) and the corresponding flow coefficient is the lowest value that can be used to maintain attached flow. Consequently, for the runs at varying angle of attack with suction, flow coefficients were maintained above these critical values. The runs without suction were made with the porous surface sealed by nonporous tape.

Standard tunnel-wall corrections were applied to the angle of attack and drag values. The increments that were added are as follows:

$$\Delta \alpha = 0.49 \text{ CL}$$

$$\Delta C_{\rm D} = 0.0085 \, {\rm C_L}^2$$

The flow coefficients were corrected for leakage which resulted from the construction of the model.

RESULTS AND DISCUSSION

Model With Undeflected Leading-Edge Flap and Tip Tanks On

The lift, drag, and pitching-moment characteristics of the model with different trailing-edge flap deflections with and without area suction applied are shown in figure 7. The force data with suction applied are shown for only one porous extent for each flap deflection. It will be noted in a later section that changing the porous extent had an effect on flap lift increment; however, the effect on the over-all characteristics of the model was small.

Lift. The force data of figure 7 show that suction increased the flap lift increments throughout the angle-of-attack range. The following table lists the measured flap lift increments and the values predicted from the potential theory of reference 11.

The predicated flap lift increment, $\Delta C_{\rm LF}$, is equal to $C_{\rm L\delta_1}({\rm d}\alpha/{\rm d}\delta)(\delta/57.3)$ where the values of $C_{\rm L\delta_1}$ and theoretical ${\rm d}\alpha/{\rm d}\delta$ of 1.86 and 0.60, respectively, were obtained from reference 11.

	$\delta_{\rm F} = 45^{\rm o}$			
	With suction	With suction		
$\left(\triangle C_{L_{\overline{F}}}\right)_{\alpha=0}$	0.85	0.96		
△CLF predicted	.88	1.07		

The fair agreement of the predicted with the measured flap lift increments at 0° angle of attack indicates that area suction was effective in essentially eliminating the separation on the flap. Tuft studies showed that some separation existed near the trailing edge of the flap with the model at 0° angle of attack. As the angle of attack was increased, this separation spread forward and there was a gradual reduction in the flap lift increment (fig. 7). The tuft studies indicated that the maximum lift coefficient with the flap deflected was limited by trailing-edge type of separation occurring on the portion of the wing outboard of the flap.

<u>Drag.-</u> Applying suction increased the drag of the model at a constant angle of attack or at a constant lift coefficient (fig. 7). However, as can be seen in the following table, suction reduced the drag coefficient per unit flap lift coefficient squared.

$$\delta_{\rm F} = 45^{\rm O} \qquad \delta_{\rm F} = 55^{\rm O}$$
 Without With without With suction suction suction
$$\left[\frac{\Delta c_{\rm D}}{(\Delta c_{\rm L_F})^2}\right]_{\alpha=0}$$
 0.29 0.18 0.30 0.19

The values of the drag parameter in this table show that suction reduced the drag caused by separation, but that this reduction in drag was overbalanced by the increased induced drag resulting from the increased lift.

Pitching moment.- The pitching-moment coefficient of the model was increased by the application of area suction to the trailing-edge flap. However, the pitching moment per unit flap lift increment at 0° angle of attack was unaffected by suction ($\Delta C_{\rm m}/\Delta C_{\rm LF}=-0.17$, with or without suction). This implies that suction had little effect on the movement of the center of pressure at 0° angle of attack.

Chordwise extent of porous area and pumping requirements. The variations of flap lift increment with suction flow coefficient for the 45° and 55° flaps were presented in figure 6 for several chordwise extents of porous area. These data show that with the smallest opening tested, an opening expected to be satisfactory on the basis of reference 1, the measured $\Delta C_{\rm LF}$ was considerably below the predicted value. Increasing the porous extent increased the measured $\Delta C_{\rm LF}$ and provided better agreement between the measured and predicted values. For this increased porous extent, the $C_{\rm QF}$ was about twice the value of $C_{\rm QF}$ predicted to be necessary by the method of reference 1. The increase in porous extent and flow coefficients required in order to obtain reasonable agreement between measured and predicted values of $\Delta C_{\rm LF}$ is believed to have been caused by the necessity of suppressing the trailing-edge separation.

In the following table, the average duct pressure coefficient measured in the trailing-edge flap duct is compared with the value predicted to be necessary from reference 1.

$$\delta_F = 45^{\circ}$$
 $\delta_F = 55^{\circ}$ with suction

P_d measured -4.5 -5.7 P_d predicted -4.7 -6.4

The measured pressures correspond to the critical flow values with the largest opening tested, and the agreement with the predicted values is considered good.

Model With Deflected Leading-Edge Flap and Tip Tanks On

The lift, drag, and pitching-moment data shown in figure 8 are for the model with the nose flap deflected, with the trailing-edge flap either undeflected or deflected 45°, and with suction applied.

Lift.- The change in $C_{I_{max}}$ obtained by deflecting the sealed nose flap was small compared to the increase in $C_{I_{max}}$ obtained with the suction nose flap. With suction applied to the nose flap, $C_{I_{max}}$ values of 2.2 and 2.5 were measured in conjunction with the undeflected and deflected suction trailing-edge flap, respectively. If the suction nose

NACA RM A57KOL

flap were as effective in controlling separation as in the swept-wing tests of references 5 and 9 and in unpublished two-dimensional tests, CLmax values of 2.4 and 3.0 would be expected with the 400 nose flap. The lower effectiveness of the suction nose flap on the present unswept wing was due to trailing-edge separation that occurred at angles of attack below those for $C_{L_{max}}$. This separation was evidenced by the $\mathtt{C}_{\mathtt{L}_{\mathtt{max}}}$ and also by the tuft studies. The nonlinear lift curve near tuft studies made with the trailing-edge flap deflected showed that separation occurred near the trailing edge of the undeflected aileron at about 10° angle of attack. At a higher angle of attack, separation was also apparent on the rearward third of the wing near the fuselage. Boundary-layer surveys indicated that the latter trailing-edge separation was aggravated by an unstable boundary layer resulting from the juncture of the nose flap and fuselage. As the angle of attack for CImax was approached, the separation on the undeflected aileron and on the portion of the wing near the fuselage spread forward and toward the center of the wing. An attempt was made to reduce this separation with the vortex generators located as shown in figure 5. As can be seen from the data of figure 9, these vortex generators reduced the separation, and the CI_{max} with the 30° nose flap was increased from 2.4 to 2.7 with the suction trailing-edge flap deflected. In addition to this increase in $C_{L_{max}}$, a nearly linear variation of lift with angle of attack was obtained. Thus, it is concluded that the maximum effectiveness of an area-suction leading-edge flap cannot be obtained if there is trailing-edge separation.

Drag and pitching moment. Applying area suction to the leading-edge flap delayed separation to higher angles of attack, and the parabolic drag variation with lift (induced drag) was extended to higher angles of attack. Deviations from this curve below $C_{\rm Imax}$ (fig. 8(a)) indicate the occurrence of trailing-edge type of separation that has been noted previously. With the trailing-edge flap undeflected, the pitching-moment variation with lift was extended linearly to the increased $C_{\rm Imax}$ by the use of the area-suction leading-edge flap. With the trailing-edge flap deflected, a nonlinear variation of pitching moment with lift was obtained with and without the leading-edge flap. For this configuration, area suction on the leading edge delayed the unstable break in pitching-moment curve to increased lift coefficients.

Pumping requirements.— It was noted previously that trailing-edge separation occurred at angles of attack below $C_{\rm Imax}$ with suction applied to the leading-edge flap. Since this separation was to some extent controlled by suction, the portion of the pumping requirements which acted only to control separation at the leading-edge flap could

not be clearly defined. For this reason, only a limited amount of data was obtained with various flow and pressure coefficients. The variation of lift coefficient with suction flow coefficient is shown in figure 10 for several angles of attack and for different nose flap deflections. Duct pressure coefficients ranging from -5 to -7 were measured at a flow coefficient of 0.001 for the configurations for which data are presented in figure 10.

Model With Tip Tanks Removed

The data obtained for various leading- and trailing-edge flap configurations with the wing tip tanks removed are presented in figure 11. Comparison of these data with those for the comparable configuration with the tanks on (figs. 7, 8, and 9) indicate that the primary effect of removing the tip tanks was a reduction in the lift curve slope of about 13 percent.

CONCLUDING REMARKS

The results of tests conducted with a straight, moderately thick wing showed that area suction increased the lift increment obtained from the trailing-edge flap throughout the angle-of-attack range. When area suction was applied to the leading-edge flap, the maximum lift coefficient was increased both with and without the trailing-edge flap deflected. However, comparison of these results with those of other tests showed that the effectiveness of area suction applied to the knee of the trailing-edge flap and/or leading-edge flap was reduced by trailing-edge air-flow separation that occurred on the wing.

Ames Aeronautical Laboratory
National Advisory Committee for Aeronautics
Moffett Field, Calif., Nov. 1, 1957

REFERENCES

- Cook, Woodrow L., Holzhauser, Curt A., and Kelly, Mark W.: The Use of Area Suction for the Purpose of Improving Trailing-Edge Flap Effectiveness on a 35° Sweptback Wing. NACA RM A53E06, 1953.
- 2. Anderson, Seth B., and Quigley, Hervey C.: Flight Measurements of the Low-Speed Characteristics of a 35° Swept-Wing Airplane With Area-Suction Boundary-Layer Control on the Flaps. NACA RM A55K29, 1956.

NACA RM A57KOL

3. Kelly, Mark W., and Tolhurst, William H., Jr.: The Use of Area Suction to Increase the Effectiveness of a Trailing-Edge Flap on a Triangular Wing of Aspect Ratio 2. NACA RM A54A25, 1954.

- 4. Griffin, Roy N., Jr., and Hickey, David H.: Investigation of the Use of Area Suction to Increase the Effectiveness of Trailing-Edge Flaps of Various Spans on a Wing of 45° Sweepback and Aspect Ratio 6. NACA RM A56B27, 1956.
- 5. Holzhauser, Curt A., Martin, Robert K., and Page, V. Robert: Application of Area Suction to Leading-Edge and Trailing-Edge Flaps on a 44° Swept-Wing Model. NACA RM A56FO1, 1956.
- 6. Koenig, David G.: The Use of Area Suction for Improving the Longitudinal Characteristics of a Thin Unswept Wing-Fuselage Model With Leading- and Trailing-Edge Flaps. NACA RM A56D23, 1956.
- 7. Koenig, David G., and Aoyagi, Kiyoshi: The Use of a Leading-Edge Area-Suction Flap and Leading-Edge Modifications to Improve the High-Lift Characteristics of an Airplane Model With a Wing of 45° Sweep and Aspect Ratio 2.8. NACA RM A57H21, 1957.
- 8. Holzhauser, Curt A., and Bray, Richard S.: Wind-Tunnel and Flight Investigations of the Use of Leading-Edge Area Suction for the Purpose of Increasing the Maximum Lift Coefficient of a 35° Swept-Wing Airplane. NACA Rep. 1276, 1956.
- 9. Holzhauser, Curt A., and Martin, Robert K.: The Use of a Leading-Edge Area-Suction Flap to Delay Separation of Air Flow From the Leading Edge of a 35° Sweptback Wing. NACA RM A53J26, 1953.
- 10. Cook, Woodrow L., and Kelly, Mark W.: The Use of Area Suction for the Purpose of Delaying Separation of Air Flow at the Leading Edge of a 63° Swept-Back Wing Effects of Controlling the Chordwise Distribution of Suction-Air Velocities. NACA RM A51J24, 1952.
- 11. DeYoung, John: Theoretical Symmetric Span Loading Due to Flap
 Deflection for Wings of Arbitrary Plan Form at Subsonic Speeds.
 NACA Rep. 1071, 1952. (Supersedes NACA TN 2278.)

TABLE I.- COORDINATES OF THE AIRFOIL SECTION - AN NACA 65_{1} -213 (a = 0.5)

[All stations and ordinates in percent chord]

Upper surface		Lower surface		
Station Ordinate		Station	Ordinate	
0 .38 .62 1.10 2.34 4.81 7.31 9.80 14.81 19.83 24.86 29.89 34.92 39.96 45.01 50.07 55.14 70.13 75.11 80.09 85.06 90.04 95.01 100.00	0 1.06 1.29 1.64 2.28 3.26 4.67 5.71 6.51 7.56 7.85 7.98 7.94 7.71 7.26 6.63 5.89 5.04 4.14 3.19 2.24 1.33 .53 0	0 .62 .88 1.40 2.66 5.19 7.69 10.20 15.19 20.17 25.14 30.11 35.08 40.04 44.99 49.93 54.86 69.87 74.89 79.91 84.94 89.97 94.99 100.00	0 92 -1.10 -1.35 -1.76 -2.38 -2.84 -3.22 -3.82 -4.59 -4.59 -4.59 -4.96 -5.01 -4.95 -4.47 -4.47 -4.07 -3.60 -3.60 -2.49 -1.88 -1.29 -1.88	

TABLE II.- COORDINATES OF TIP TANKS

Station, in.	Radius, in.
0	0
10	7.4
20	10.8
30	12.4
40	12.8
90 ^a	12.8
120	12.8
130	12.0
140	10.1
160	5.7

aTip tank station at 52 percent chord station of wing.

TABLE III.- COORDINATES OF FUSELAGE

Fuselage station, in.	ion, center line, center line,		Width, in.	
0 20 40 60 90 120 150 180 210 230 288 335 380 425 484	0 14.0 19.6 23.2 27.0 40.2 50.0 48.2 42.4 36.0 33.4 32.0 29.2 25.6 18.2	0 14.0 19.6 23.2 27.0 30.0 32.0 33.2 33.8 34.0 33.2 31.4 28.6 25.0 19.4	0 28.0 36.0 41.2 46.8 50.0 52.4 53.4 54.0 53.4 47.6 43.0 36.0	

TABLE IV.- CONFIGURATIONS TESTED

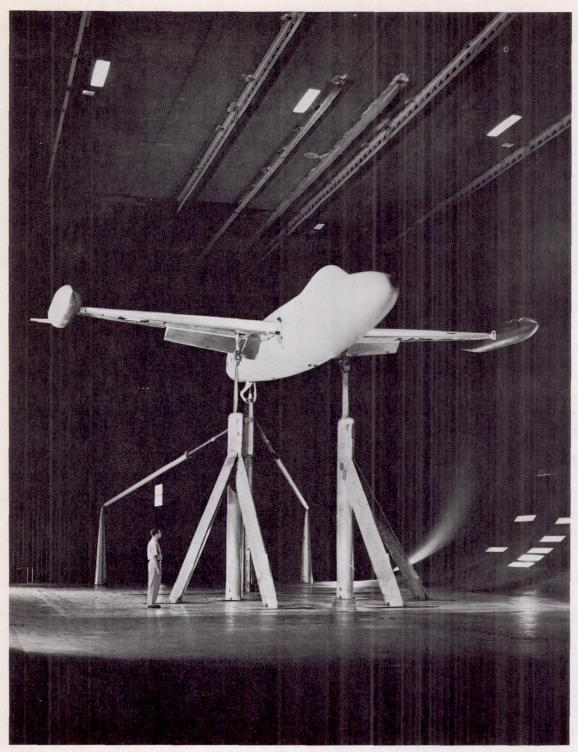
		ous area		Porous area			
$\delta_{ m F},$ deg	Forward edge, percent chord	Total open- ing, percent chord	δ _N , deg	¹ Forward edge, percent chord	Total open- ing, percent chord	Tip tanks	Comments
-	CHOIG			CHOIG			
0			0			On	
45	1.2 1.2 1.2	sealed 2.5 3.8 6.3					
55	1.1 1.1 1.1	sealed 3.8 4.9 6.0					
0			20 20 40 40	 0.7 .7	sealed 2.3 sealed 3.8		
45	1.2	3.8	20 20 30 30 40	 .7 .7	sealed 2.3 sealed 3.0 3.8		(2,3)
0			0			Off	
45	1.2	sealed 3.8	30 30	 -7	sealed		(3)

Distance ahead of midarc, see figure 3.

This configuration also tested with inboard row of vortex generators, see figure 5.

This configuration also tested with inboard and outboard rows of vortex generators, see figure 5.

15



A-20674

Figure 1.- The model with flaps deflected in the Ames 40- by 80-foot wind tunnel.

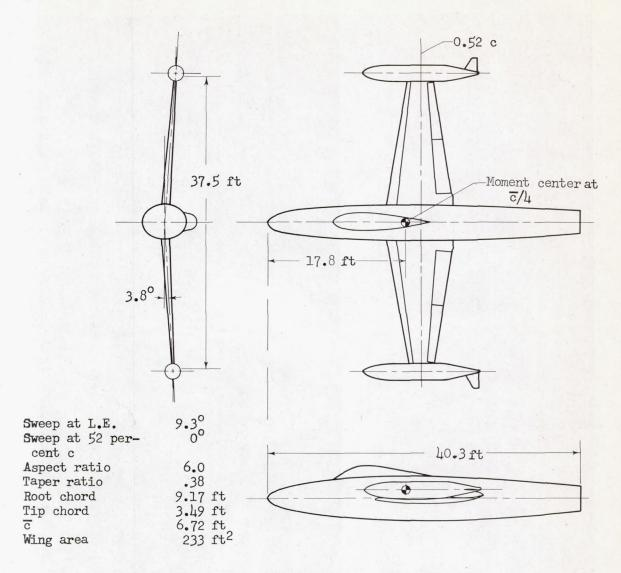


Figure 2.- Three-view drawing of the model.

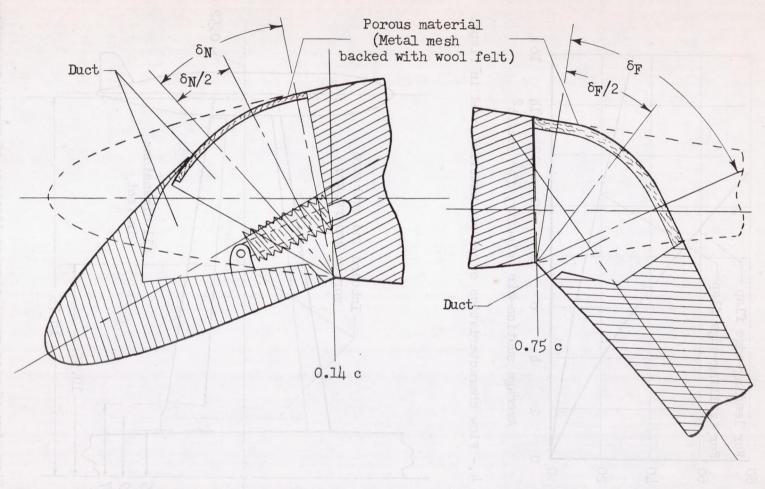


Figure 3.- Details of the leading-edge and trailing-edge flaps; $\delta_{\rm N}$ = 30°, $\delta_{\rm F}$ = 55°.

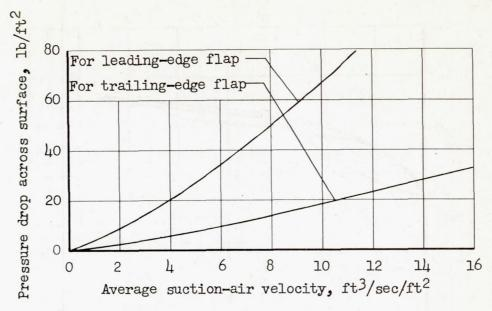


Figure 4.- Flow characteristics of porous material used in flaps.

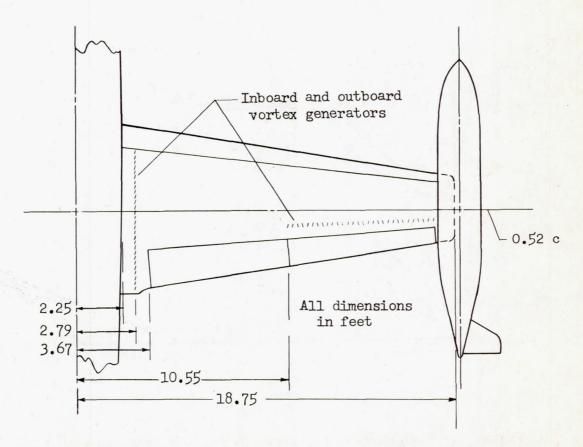
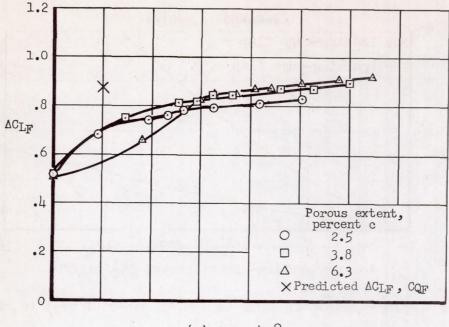
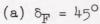
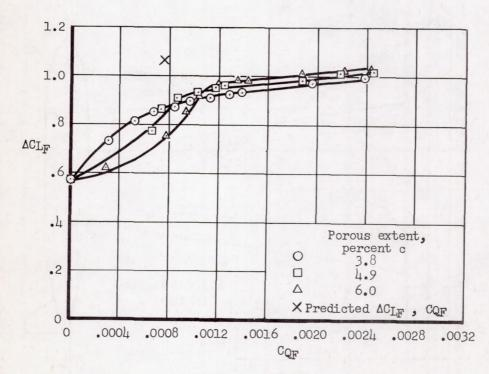


Figure 5.- Plan view of wing panel showing location of vortex generators.







(b) $\delta_{\rm F} = 55^{\rm o}$

Figure 6.- Suction flow requirements for the trailing-edge flap; α = 0°, δ_N = 0°, tip tanks on.

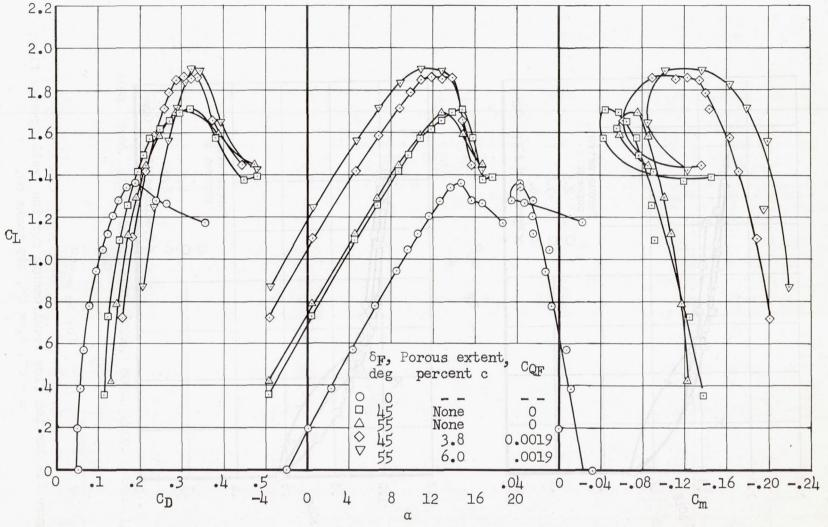


Figure 7.- Aerodynamic characteristics of model with several trailing-edge flap configurations; $\delta_{\mathbb{N}}$ = 0°, tip tanks on.

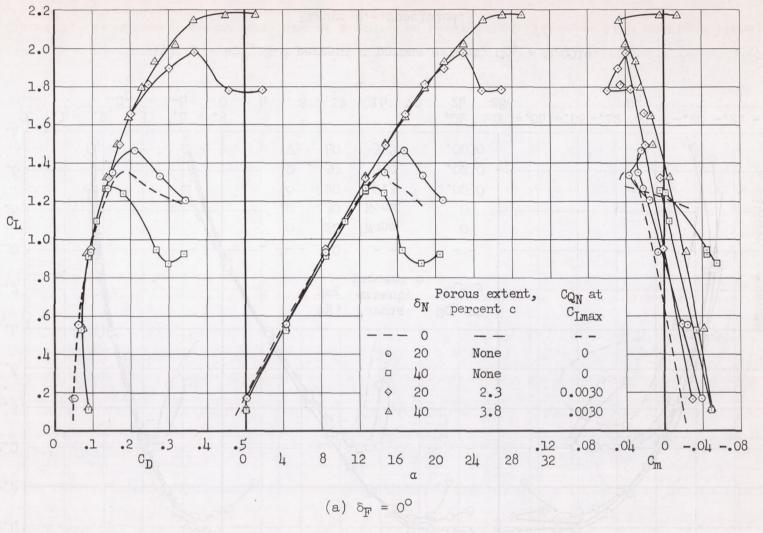
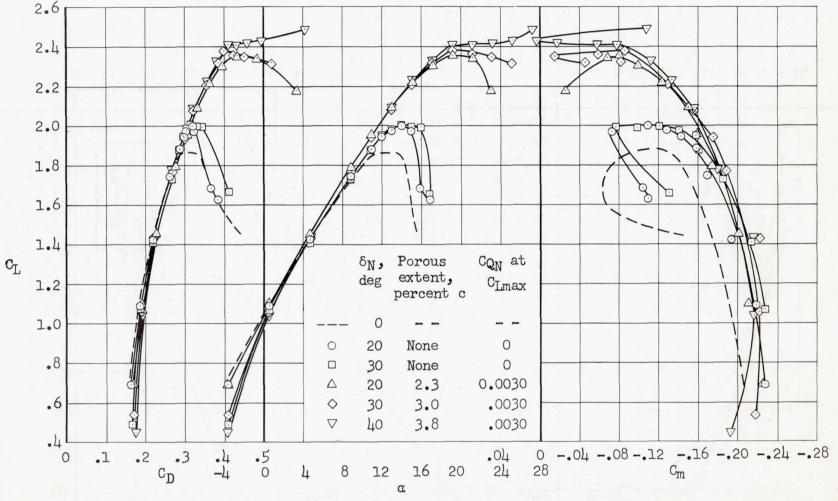


Figure 8.- Aerodynamic characteristics of model with several nose flap configurations; tip tanks on.



(b) $\delta_{\rm F} = 45^{\circ}$, 3.8 percent c porous extent, $C_{\rm Q_F} = 0.0019$.

Figure 8.- Concluded.

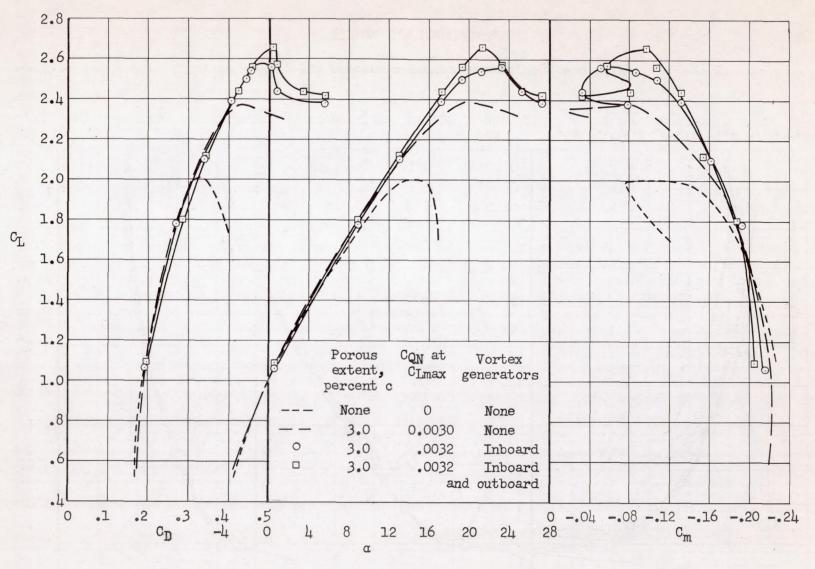


Figure 9.- Effect of vortex generators on characteristics of model with nose flap deflected 30°; $\delta_{\rm F}$ = 45°, 3.8 percent c porous extent, $C_{Q_{\rm F}}$ = 0.0019, tip tanks on.

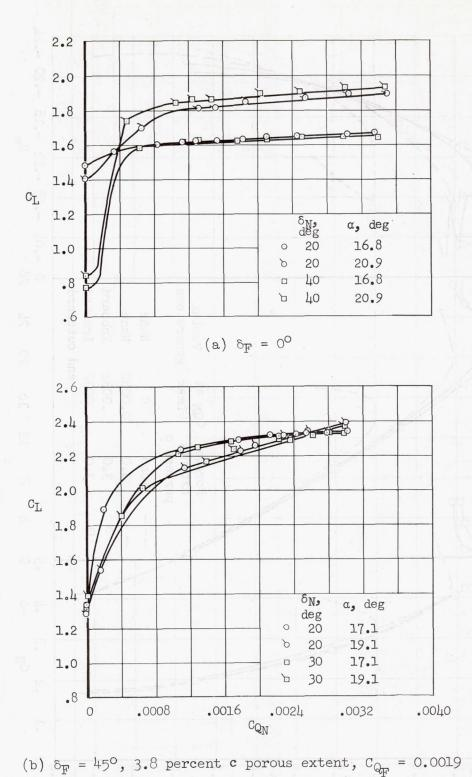


Figure 10.- Suction flow requirements of leading-edge flap; tip tanks on.

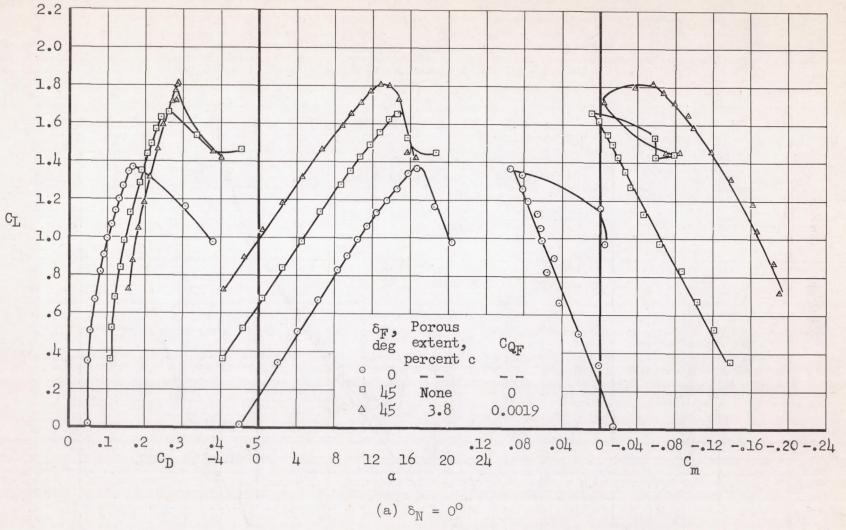
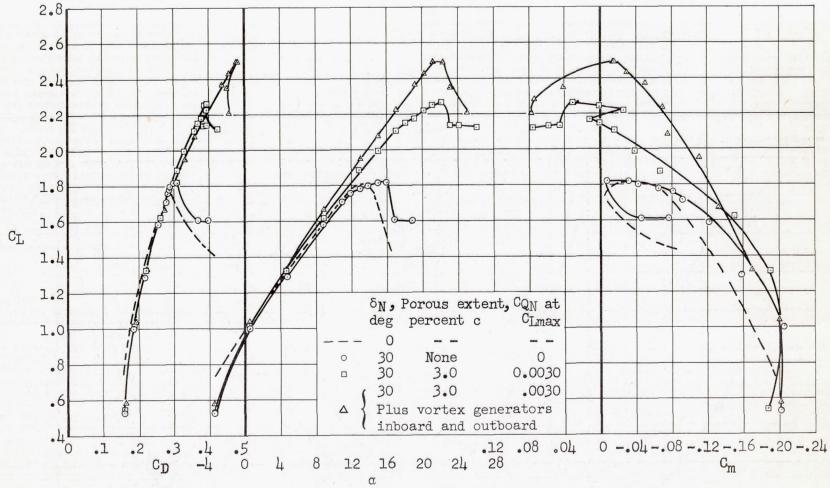


Figure 11.- Aerodynamic characteristics of model with tip tanks removed.



(b) $\delta_{\rm N}$ = 30°; $\delta_{\rm F}$ = 45°, 3.8 percent c porous extent, $C_{\rm QF}$ = 0.0019

Figure 11. - Concluded.